

Effect of a Polar Environment on the Conformation of Phospholipid Head Groups Analyzed with the Onsager Continuum Solvation Model

Johan Landin[†] and Irmin Pascher^{*‡}

Department of Medical Biochemistry and MEDNET Laboratory, Göteborg University, Medicinaregatan 9, S-413 90 Göteborg, Sweden

Dieter Cremer[§]

Department of Theoretical Chemistry, Göteborg University, Kemigården 3, S-412 96 Göteborg, Sweden

Received: June 5, 1996; In Final Form: October 25, 1996[⊗]

The effect of the polarity of the environment on the conformation of the zwitterionic membrane lipid head groups phosphoethanolamine (PE) and phosphocholine (PC) has been investigated with calculations at the Hartree–Fock level using the 3-21G(*), 6-31G*, and 6-31+G* basis sets together with the Onsager continuum solvation model. Results suggest that in the gas phase both PE and PC adopt cyclic minimum energy conformations, in which an ammonium or *N*-methyl hydrogen closely approaches one of the nonesterified phosphate oxygens. In the case of PE, intramolecular interactions result in a proton transfer from the ammonium group to the phosphate oxygen, which however is suppressed by a moderate increase in the polarity of the surrounding medium. With increasing polarity of the environment, the cyclic structures of PE and PC still remain low-energy conformers but simultaneously for both head groups an almost identical extended conformer, typical of crystal structures, becomes increasingly favored. Already at $\epsilon = 10$, the extended conformer of PC is favored (−2.4 kcal/mol) relative to the cyclic one, while for PE the relative energy of the extended conformer approaches that of the cyclic one at $\epsilon = 80$. The similarity and increasing stability of the extended PE/PC conformers in the monomeric state and the fact that this conformer is also adopted in all crystal structures of PE/PC lipids, regardless of hydration and interaction pattern, indicate that the geometry of this conformer is determined by energetics intrinsic to the phosphoethanolammonium backbone. In lipid aggregates or a membrane environment the extended conformer becomes additionally stabilized by intermolecular ionic and hydrogen bond interactions with neighboring molecules substituting for the internal interaction that in the monomeric state constrains the zwitterionic dipole into a cyclic structure.

1. Introduction

Zwitterionic phosphoethanolamine (PE) and the corresponding fully *N*-methylated phosphocholine (PC) are the most abundant head groups of amphipathic lipid constituents of biological membranes.¹ Although the two head groups are structurally and chemically closely related, the two lipid types, phosphatidylethanolamine and phosphatidylcholine, exhibit remarkable differences with respect to their structural properties and their distribution in membrane bilayers. In aqueous dispersions phosphatidylcholine forms lamellar bilayer arrangements, in both the crystalline and liquid-crystalline phase,^{2,3} while phosphatidylethanolamine in the liquid-crystalline state converts into inverted hexagonal (H_{II}) structures^{4–6} and requires the admixture of other lipids to retain a lamellar bilayer arrangement. In plasma membranes, phosphatidylcholine is located predominantly in the outer leaflet, while phosphatidylethanolamine is found in the inner leaflet of the bilayer only.⁷ This asymmetric distribution is maintained by an ATP-dependent protein which specifically translocates phosphatidylethanolamine (and phosphatidylserine) to the inside of the plasma membrane.⁸

Despite extensive studies in many laboratories, the specific role of phosphatidylethanolamine and phosphatidylcholine and

the significance of their asymmetric distribution for the structure and function of biomembranes are still poorly understood. On a molecular level it has been of interest to explore to what extent PE and PC head groups differ with respect to molecular conformation, lateral interactions, and dipole arrangements and how these features affect the properties and topology of the membrane surface. Pascher and co-workers⁹ studied these aspects by single-crystal analyses of a number of phosphoethanolamine lipids and polar constituents with different degrees of *N*-methylation and hydration. A comparative analysis of 13 different PE/PC structures⁹ results in the following conclusions:

(i) In all crystal structures the zwitterionic PE/PC head groups adopt a characteristic, rather extended conformation in which the (+) charged nitrogen atom is located within a narrow sector with respect to the phosphate ester oxygen. (Figures 1 and 2, Table 1). (ii) Surprisingly this conformation is not affected by the number of *N*-methyl groups or by hydration of the phosphate group. (iii) It is also not affected by the packing arrangement of the P–N dipoles (P = phosphorus, N = nitrogen), although the lateral interactions and packing pattern of the P–N dipoles show large variations and crucial differences for PE and PC compounds.

The conformational features observed in crystal structures are also supported by NMR studies of PE/PC lipids in aqueous dispersions and natural membrane systems¹⁰ showing that a preferred conformation is predominant also in dynamic systems. This indicates that the conformation of the zwitterionic phosphoethanolamine/phosphocholine group is determined by strong

[†] Johan.Laudin@medkem.gu.se.

[‡] Irmin.Pascher@medkem.gu.se.

[§] Cremer@oc.chalmers.se.

[⊗] Abstract published in *Advance ACS Abstracts*, March 15, 1997.

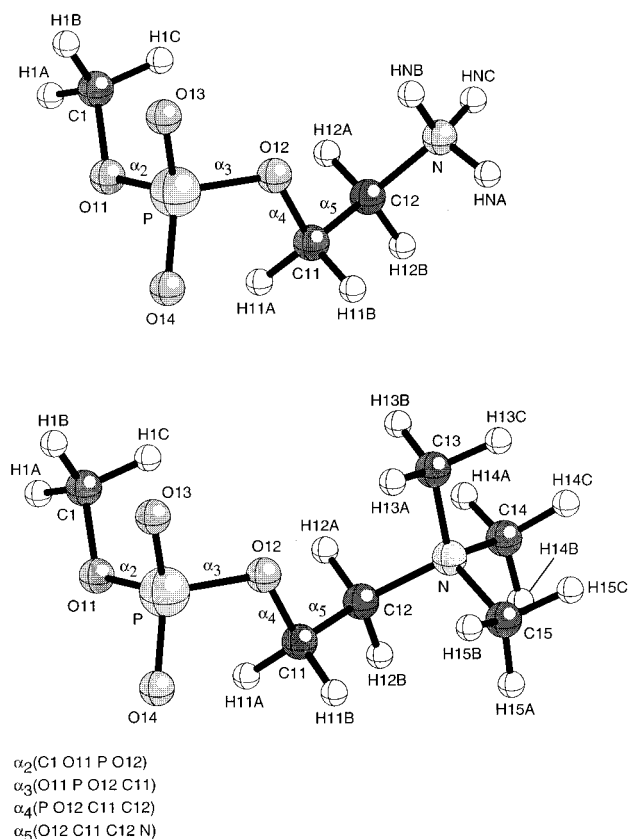


Figure 1. Atom labeling and dihedral angle notation for the phosphoethanolamine (PE) and phosphocholine (PC) head groups.

intramolecular forces. The energetics giving rise to this preferred conformation, however, is still not satisfyingly explained in quantum chemical terms.

Using theoretical calculations, Pullman^{11–13} and Frischleder^{14,15} earlier demonstrated that under gas-phase conditions a cyclic minimum energy conformation is obtained, which will change to a more extended one if hydration¹² or the presence of neighboring head groups¹⁵ is taken into account. The experimental data show that the conformation is largely independent of the hydration state and head group packing patterns, i.e. that not specific interactions with neighboring molecules but rather the overall polarity of the environment affects the conformation of the PE/PC dipole. Recently, Woolf and Roux,¹⁶ using empirical force-field methods, have shown that the potential energy surface of PE/PC head groups is significantly affected by the polarity of the surroundings.

We have earlier applied quantum chemical methods in conformational studies of the two PE head group substructures, dimethylphosphate (DMP) and 2-ammonioethanol (AME) and shown that the gas-phase minimum energy geometries of these head group fragments correspond well to the preferred conformation observed in crystals.¹⁷ In the present work we have extended our ab initio calculations to determine minimum energy conformations of the entire PE and PC head groups. Furthermore, to explore the effects of the polarity of the environment on the head group minimum energy conformations, we have performed calculations according to the continuum solvation model by Onsager.^{18–21} It is clear that a realistic description of the intermolecular interactions occurring in the hydrated bilayer should include three different effects, namely, (1) the intramolecular electronic effects (determining the conformation of the head group in the gas phase), (2) the intermolecular interactions between neighboring head groups in the bilayer, and (3) the interactions between head groups and water

molecules. Hence, to describe all effects, one should consider a model with at least two neighboring head groups located in a continuum with the dielectric constant of water. Since such an investigation was not feasible, we have used a more simplified model in which effects 2 and 3 were covered by a continuum description with a dielectric constant typical for the interface region of membrane bilayers. By this simplification the description of the conformation of the polar head groups becomes a computationally accessible problem even though some of the conclusions drawn from this description have to be considered with care.

2. Methods and Notations

Computational Methods. All calculations were done with the Gaussian 90/92^{22,23} and COLOGNE94²⁴ ab initio packages at the Hartree–Fock (HF) level of theory. Three basis sets of DZ+P quality were used, namely, the 3-21G(*),^{25–27} 6-31G*,^{28–31} and 6-31+G*^{28–32} basis sets of Pople and co-workers.

Geometry optimizations for molecules in the gas phase were carried out without any constraints. Conformers in the crystal state were modeled by freezing the conformation in question, i.e. its dihedral angles as determined by the X-ray structural analysis, and then optimizing all remaining geometrical parameters such as bond lengths and bond angles. All conformations discussed in this work were optimized to obtain comparable energies. In some cases, geometry optimizations were repeated to consider solvent effects on geometry and conformation dependence on the polarity of the surroundings (see below).

Solvent Model. For the simulation of a polar environment the Onsager self-consistent reaction field (SCRf) model^{18–21} was used as implemented in Gaussian 92. In the Onsager method, the solute molecule is placed in a spherical cavity surrounded by a continuum with constant dielectric properties. The equilibrium geometry is rather sensitive to the cavity radius used, and therefore the cavity was recalculated after the first geometry optimization and the molecule reoptimized with the new value. The procedure was repeated until a consistent radius was obtained, and this cavity radius was then kept fixed for all conformers investigated in addition to the equilibrium conformation. Only the electrostatic effects of solvation are included in the Onsager model, and other forces such as cavity work, dispersion, or exchange repulsion effects are neglected. This is a reasonable approximation when zwitterions or strongly polar molecules are studied in polar solvents where the electrostatic effects of solvation are expected to be predominant.³³ The total energy of solute and solvent, which depends on the dielectricity constant ϵ , is denoted as E_s (for a general description of solvation energies, see refs 34 and 35). Partial atomic charges in a polar surrounding were calculated according to the CHELPG charge partitioning scheme.³⁶

Bond Characteristics. To investigate bonding properties, a bond electron density analysis was carried out using COLOGNE94. Thus, the electron density distribution $\rho(\mathbf{r})$ and the energy density distribution $H(\mathbf{r})$ were used for characterizing individual bonds as covalent or electrostatic according to the criteria given by Cremer and Kraka.³⁷ For both covalent and electrostatic bonds, the atoms in question are connected by a path of maximum electron density characterized by a bond critical point. The energy density is negative (stabilizing) at the bond critical point in the case of a covalent bond, while it is close to zero or positive (destabilizing) in the case of an electrostatic bond.³⁷ In the case of an electrostatic bond, energy density and electron density at the bond critical point reveal how much the electrostatic bond differs from a true covalent bond.

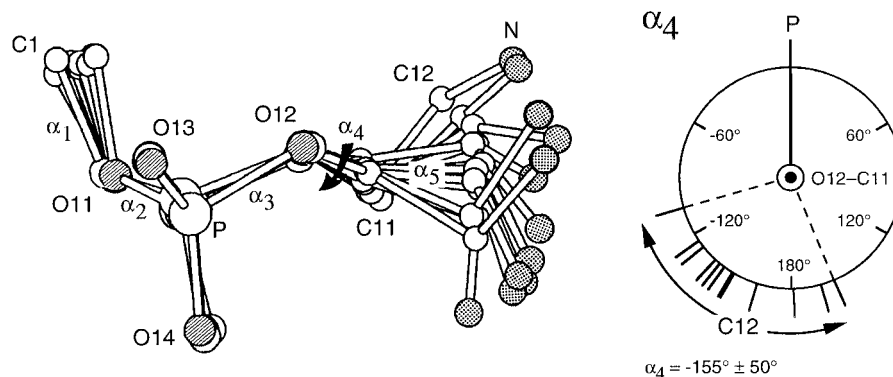


Figure 2. Preferred conformations of the phosphoethanolammonium group in crystal structures.⁹ The head groups of 12 different phosphoethanolammonium compounds with varying degree of *N*-methylation have been superimposed with best fit for the α -chain from atom C(1) to C(11). The shown phosphoethanolammonium groups are the $-\alpha$ conformers (Table 1, left column). Another 12 phosphoethanolammonium head groups with the corresponding $+\alpha$ mirror image conformation (Table 1, right column) are not shown.

TABLE 1: Preferred Conformations of Phosphoethanolamine Head Groups Observed in Crystal Structures^a

no.	compound abbr ^b	chir	image					abbr	mirror image				
			α_1	α_2	α_3	α_4	α_5		α_1	α_2	α_3	α_4	α_5
1	PPE	<i>rac</i>	-94	-60	-71	157	60	PPE	94	60	71	-157	-60
2	GPE	<i>sn</i>	-174	-81	-81	164	55	GPE					
3	GPC CdCl ₂	<i>sn</i>	169	-69	-73	178	73	GPC CdCl ₂					
4	OMPC	<i>sn</i>						OMPC	-166	68	67	173	72
5	PPEM ₂	<i>rac</i>	174	-61	-64	-163	55	PPEM ₂	-174	61	64	163	-55
6	DMPC B	<i>sn</i>	177	-74	-47	-150	54	DMPC A	163	62	68	143	-64
7	PPC B	<i>sn</i>	168	-76	-59	-149	72	PPC A	156	53	70	144	-77
8	DLPEM ₂	<i>rac</i>	-179	-65	-54	-144	96	DLPEM ₂	179	65	54	144	-96
9	HPC B	<i>sn</i>	167	-69	-56	-141	69	HPC A	-161	61	64	138	-69
10	GPC A	<i>sn</i>	165	-71	-59	-138	73	GPC B	-172	64	65	140	-75
11	deoxyLPC		-162	-86	-45	-129	-89	deoxyLPC	162	86	45	129	84
12	DLPEM ₁	<i>rac</i>	174	-61	-60	-125	59	DLPEM ₁	-174	61	60	125	-59
13	DLPE	<i>rac</i>	154	-58	-66	-106	-67	DLPE	-154	58	66	106	67

^a Torsion angles of head groups of phospholipids and phospholipid components with varying degree of *N*-methylation are compiled with respect to their α_2/α_3 torsion angles ($-/-$ or $+/+$) and to increasing/decreasing torsion angle α_4 . For notation of torsion angles and conformational drawings see Figures 1 and 2. The table comprises racemates (*rac*) and natural enantiomers (*sn*) with respect to the configuration of the chiral glycerol carbon atom C(2). In crystals the racemates display a packing pattern in which the head groups adopt mirror image conformers with crystallographic centrosymmetry. The coexistence of mirror image conformers is also observed for the head groups of most of the enantiomers, but in these cases the conformers are related by a noncrystallographic mirror symmetry (cf. compounds 6, 7, 9, 10; left and right table). ^b Systematic names of phosphoethanolamine head groups: PPE, 1-palmitoyl-*rac*-glycero-3-phosphoethanolamine; GPE, *sn*-glycero-3-phosphoethanolamine monohydrate; GPC CdCl₂, *sn*-glycero-3-phosphocholine cadmium chloride trihydrate; OMPC, 1-octadecyl-2-methyl-*sn*-glycero-3-phosphocholine monohydrate; PPEM₂, 1-palmitoyl-*rac*-glycero-3-phospho-*N,N*-dimethylethanolamine; DMPC (A+B), 1,2-dimyristoyl-*sn*-glycero-3-phosphocholine dihydrate; PPC (A+B), 1-palmitoyl-*sn*-glycero-3-phosphocholine monohydrate; DLPEM₂, 1,2-dilauroyl-*rac*-glycero-3-phospho-*N,N*-dimethylethanolamine; HPC (A+B), 1-hexadecyl-*sn*-glycero-3-phosphocholine chloroform solvate; GPC (A+B), *sn*-glycero-3-phosphocholine; deoxyLPC, 1-lauroyl-2-deoxyglycero-3-phosphocholine monohydrate; DLPEM₁, 1,2-dilauroyl-*rac*-glycero-3-phospho-*N*-monomethylethanolamine; DLPE, 1,2-dilauroyl-*rac*-glycero-3-phosphoethanolamine acetic acid.

Notations. Atom numbering and dihedral angle notations are according to Sundaralingam³⁸ (cf. Figure 1). To distinguish different compounds and conformers, the following notation is used: each molecule is first identified by the abbreviation of its systematic name, i.e. PE or PC. Further, a suffix identifies the conformer with respect to the environment and geometry: "gas" refers to conformers minimized in the gas phase, "solcyc" (cyclic) and "solext" (extended) is used for conformers optimized in a polar environment. Throughout this paper the term "extended" is used for the "noncyclic" P-N zwitterion conformation characteristically observed in crystal structures and in structure optimizations in a polar medium (cf. Figures 2, 6, and 7). Thus "extended" does not necessarily imply a fully antiperiplanar conformer.

Other primary suffixes, using the abbreviations of the phospholipids listed in Table 1, denote conformers with dihedral angles locked at values of the corresponding crystal structure. Finally, fully optimized conformers are characterised by a secondary suffix denoting the level of theory used, e.g. HF3, HF6, and HF6+ refer to the methods HF/3-21G(*), HF/6-31G*, and HF/6-31+G*, respectively.

3. Results and Discussion

In Table 1, dihedral angles of a number of PE and PC conformations determined in the crystal state are listed. Calculated dihedral angles of conformations as obtained for different basis sets are given in Table 2. Table 3 summarizes results of the analysis of the electron density distribution for cases of close contact between nonbonded atoms, while Tables 4 and 5 list dihedral angles and relative energies of cyclic and extended conformations showing their dependence on the polarity of the environment.

3.1. Geometry Optimization of PE and PC Head Groups in the Gas Phase. PE and PC head groups from two representative crystal structures, namely, *sn*-glycero-3-phosphoethanolamine monohydrate (GPE)³⁹ and 1,2-dimyristoyl-*sn*-glycero-3-phosphocholine dihydrate (DMPC),⁴⁰ were chosen as starting structures for gas-phase optimizations. Hydrogen atoms were added to the crystal coordinates, and by keeping all other parameters locked, the hydrogen positions were optimized at the HF/3-21G(*) level. In the following steps, all parameters except the dihedral angles α_2 , α_3 , α_4 , and α_5 were optimized at

TABLE 2: Dihedral Angles and Gas-Phase Energies of the Two Crystal Conformers (PE_{GPE} and PC_{DMPC B}) Compared to the Corresponding Gas-Phase Values of the Head Group Fragments Dimethylphosphate (DMP) and Ammonioethanol (AME) as Well as the Complete Zwitterionic Phosphoethanolamine (PE) and Phosphocholine (PC) Head Groups^a

conformer	α_2	α_3	α_4	α_5	relative energy
A					
PE _{GPE}	-81.1	-81.2	163.8	55.5	0.0
DMP _{gasHF6}	-75.1	-75.1			-0.1
AME _{gasHF6}			173.3	48.5	-0.4
PE _{gasHF3}	-103.0	-59.6	-95.5	74.0	-27.0
PE _{gasHF6}	-84.4	-65.6	-96.2	72.7	-22.2
rPE _{gasHF6+}	-86.5	-65.0	-93.6	75.1	-20.9
rPE _{gasHF6+}	-99.3	-36.7	-96.2	70.4	-36.7
B					
PC _{DMPC B}	-74.0	-47.0	-150.0	54.0	0.0
PC _{gasHF3}	-88.8	-113.4	-113.1	61.6	-7.8
PC _{gasHF6}	-77.9	-104.9	-117.2	62.9	-4.9
PC _{gasHF6+}	-79.7	-100.6	-118.1	64.3	-4.6

^a Dihedral angles α_i in degrees; relative energies in kcal/mol with the crystal conformer as reference point. Absolute energies are listed in the Supporting Information.

the same level of theory, and finally, all constraints were released to allow a global optimization. For optimizations at higher levels of theory, the conformer calculated at the lower level was used as a starting point.

In a previous paper, we investigated the conformational potential energy surfaces of two fragments of the PE head group, namely, the dimethylphosphate anion (DMP) and the 2-ammonioethanol cation (AME),¹⁷ assuming that preferred conformational features are largely additive in molecules apart from coupling effects between directly adjacent rotor groups. Indeed, gas-phase optimization of the DMP and AME fragments at the HF/6-31G* level of theory resulted in dihedral values very close to those of the GPE crystal structure (see Table 2 and Figure 3). However, optimization of the whole PE head group leads to a different geometry, in which the molecule adopts a cyclic conformation. The large structural change is due to a very strong attraction between the (+) charged ammonium group and a (-) charged phosphate oxygen atom (O14). In the gas phase this strong attraction actually causes a proton of the ammonium nitrogen to jump to the phosphate oxygen, thus converting the zwitterion to a neutral molecule denoted as rPE (r stands for reaction, see Figure 4). This H⁺ transfer was found at all levels of theory investigated in this work.

To avoid the H⁺ transfer and to retain a zwitterionic nature of the PE head group comparable with its state in crystal structures and aqueous environments, the N-H bond was locked at a distance typical for the applied level of theory and the molecule reoptimized. This procedure resulted again in a cyclic conformation that is 15.8 kcal/mol higher in energy (HF/6-31+G*) than the rPE structure but 20.9 kcal/mol lower than the extended conformer found in the crystal. Compared to the extended PE conformer the cyclic conformer is formed mainly by a 100° rotation about the O12-C11 bond, changing α_4 from 163.8° (PE_{GPE}) to -93.6° (PE_{gasHF6+}, Table 2). The two cyclic conformers, with and without H⁺ transfer, are rather similar in geometry. The most significant change is that α_3 decreases from -65.0° (PE_{gasHF6+}, Table 2 and Figure 3) to -36.7° (rPE_{gasHF6+}, Table 2 and Figure 4). Furthermore, the O...H and H-N distances are 1.556 and 1.007 Å in PE_{gasHF6+}, while the O-H and H...N distances in rPE_{gasHF6+} become 0.966 and 1.908 Å, respectively. The latter is a very short distance compared to the sum of the van der Waals radii⁴¹ of hydrogen (1.2 Å) and nitrogen (1.55 Å) of 2.75 Å. The bond analysis (Table 3) shows that this is more than a pure electrostatic interaction but much

less than the covalent bonding between hydrogen and oxygen in the rPE conformer. Adding polarization functions to the hydrogen atoms, i.e. replacing the HF/6-31+G* basis with HF/6-31+G**, did not significantly change either geometry or relative energy of the rPE conformer. Finally, the influence of electron correlation on the rPE and PE conformers was checked by single-point calculations using second-order Møller-Plesset (MP2) perturbation theory.⁴² Also with electron correlation included the reaction product rPE remained the favored gas-phase conformation, although the energy difference changed from 15.8 kcal/mol (HF/6-31+G*) to 10.4 kcal/mol (MP2/6-31+G**/HF/6-31+G*) in favor of the constrained gas-phase structure PE_{gas}.

In the case of PC the cationic part is much bulkier due to the three *N*-methyl groups. However, the gas-phase optimization of PC also generated a cyclic conformer (Figure 5). Because of methyl substitution, a H⁺-transfer reaction is not favorable and, therefore, is not found in the gas-phase optimization. The optimized cyclic conformer is stabilized by electrostatic attractions between hydrogens of the choline methyl groups and the phosphate oxygen atoms, giving rise to C-H...O distances that are considerably shorter than normal van der Waals contacts (2.72 Å). Such internal interactions exist also in the PC_{DMPC B} crystal structure, where one *N*-methyl hydrogen is at a distance of 2.172 Å from a nonbonded phosphate oxygen and another hydrogen 2.161 Å from the ester oxygen atom (see Figure 5). In the crystal environment, there are also intermolecular electrostatic interactions beside the intramolecular ones. The transformation to the gas-phase conformation is mainly obtained by a concerted change of two bond torsion angles: α_3 changes from a (-) synclinal (-47°) to a (-) anticlinal position (-100.6°), which somewhat stretches the molecule (Figure 5). Simultaneously α_4 changes from nearly antiperiplanar (150°) to a (-) anticlinal position (-118.1°), by moving two hydrogen atoms of *N*-methyl groups toward the two nonbonded phosphate oxygens. The cyclic structure is stabilized by three close contacts of *N*-methyl hydrogens interacting with phosphate oxygens. One of these hydrogens is interacting with a nonesterified oxygen in a similar way as in the crystal structure (H15B). In the gas phase this distance is 2.063 Å, which is actually a little shorter than in the crystal structure and 0.657 Å shorter than the sum of the van der Waals radii (2.72 Å) of oxygen plus hydrogen. The bond analysis (Table 3) reveals that this is an electrostatic attraction of the same type as found in the rPE conformer. The other hydrogen (H13A) interacts with both a nonbonded oxygen (O13) at 2.314 Å and the phosphate ester oxygen (O12) at 2.399 Å, causing a slight asymmetry in the cyclic structure (see Figure 5). From the bond analysis it is concluded that the two latter interactions are of purely electrostatic nature. Compared to the PE case the structural differences of the PC gas-phase and crystal conformers are less significant, which is reflected by a smaller energy difference (4.6 kcal/mol, HF/6-31+G*) between the two conformers.

3.2. Geometry Optimizations of PE and PC with Dependence on ϵ . Geometry optimizations of PE and PC head groups in a polar environment generated two minimum energy conformers possessing cyclic and extended geometries, respectively, depending on the choice of starting geometry. When crystal coordinates of PE_{GPE} and PC_{DMPC B} are used as starting geometries for minimizations at $\epsilon = 10$, both structures converge to nearly identical extended conformers (Table 4 and Figures 6 and 7). The only significant difference concerns dihedral angle α_5 , which differs by approximately 10° for the two compounds. To achieve this similarity in the theoretical calculations, it is

TABLE 3: Electron Density Analysis of Ring-Closing Interactions in Gas-Phase Structures of the Phosphoethanolamine (PE) and Phosphocholine (PC) Head Groups^a

conformer	atoms	distance	type of critical point	$\rho(\mathbf{r}_b)$	$H(\mathbf{r}_b)$	character	
A	rPE _{gasHF6+}	HNA, N	1.908	(3, -1)	0.23	-0.01	electrostatic
	rPE _{gasHF6+}	HNA, O14	0.966	(3, -1)	2.22	-3.8	covalent
B	PC _{gasHF6+}	H15B, O14	2.063	(3, -1)	0.15	-0.01	electrostatic
	PC _{gasHF6+}	H13A, O13	2.314	(3, -1)	0.09	0.00	electrostatic
	PC _{gasHF6+}	H13A, O12	2.399	(3, -1)	0.09	0.01	electrostatic
	PC _{gasHF6+}	H13A, C13	1.075	(3, -1)	2.01	-2.26	covalent

^a Bond data at the HF/6-31+G* level of theory. Distance in Å, electron density distribution $\rho(\mathbf{r}_b)$ in electron Å⁻³, and energy density distribution $H(\mathbf{r}_b)$ in hartree Å⁻³. The type of each critical point \mathbf{r}_b is characterized by (rank, signature), and the character of the bond is given according to the criteria of Cremer and Kraka.³⁷

TABLE 4: Dihedral Angles of the Phosphoethanolamine (PE) and Phosphocholine (PC) Head Groups Optimized at $\epsilon = 10$ Using the Onsager Solvation Model at the HF/3-21G(*), HF/6-31G*, and HF/6-31+G* Levels of Theory^a

conformer	cavity radius	α_2	α_3	α_4	α_5	
A	PE _{solextHF3}	4.23	-61.3	-106.8	152.4	46.7
	PE _{solextHF6}	4.31	-70.9	-75.8	151.6	53.6
	PE _{solextHF6+}	4.30	-70.9	-75.9	149.6	56.2
B	PC _{solextHF3}	4.64	-68.7	-62.1	-142.7	57.9
	PC _{solextHF6}	4.73	-71.4	-75.3	152.6	64.1
	PC _{solextHF6+}	4.76	-71.8	-75.4	152.3	67.0

^a Cavity radius in Å and dihedral angles α_i in degrees.

TABLE 5: Dihedral Angles and Relative Energies at Different Dielectric Constants for the Phosphoethanolamine (PE) and Phosphocholine (PC) Head Groups Optimized Using the Onsager Solvation Model^a

dielectric const	α_2	α_3	α_4	α_5	ΔE_s
Extended Conformer					
A PE _{solextHF6+}					
10	-71.0	-75.9	150.0	55.9	5.5
20	-69.7	-75.9	145.4	61.2	3.4
30	-69.2	-75.9	143.8	63.6	2.6
40	-68.9	-75.9	143.0	64.9	2.2
80	-68.5	-75.9	141.9	66.9	1.6
B PC _{solextHF6+}					
10	-71.8	-75.4	152.3	67.0	-2.3
Cyclic Conformer					
A PE _{solcycHF6+}					
10	-74.6	-57.6	-86.2	78.6	
20	-73.4	-57.5	-85.9	79.0	
30	-73.0	-57.4	-85.8	79.1	
40	-72.7	-57.4	-85.8	79.2	
80	-72.4	-57.4	-85.7	79.3	
B PC _{solcycHF6+}					
10	-73.5	-61.1	-132.6	72.9	

^a Dihedral angles α_i in degrees, ΔE_s in kcal/mol with the cyclic conformer as reference point, all data at the HF/6-31+G* level of theory, the cavity radius was 4.31 Å (PE) and 4.76 Å (PC), respectively. Absolute energies are listed in the Supporting Information.

necessary to apply at least the HF/6-31G* level of theory. The simpler HF/3-21(*) method generates PE and PC geometries with rather different dihedral angles (Table 4). Addition of diffuse functions to the HF/6-31G* basis does not significantly affect the optimized geometry, but significantly lowers the conformational energy. Since it is well-known that diffuse functions are necessary for a reliable description of an anionic group,^{32,43,44} the HF/6-31+G* basis was used for all calculations of minimum energy conformers in the presence of a polar surrounding.

When the cyclic gas-phase conformer PE_{gasHF6+} is used as the starting geometry, optimizations at different ϵ values generate

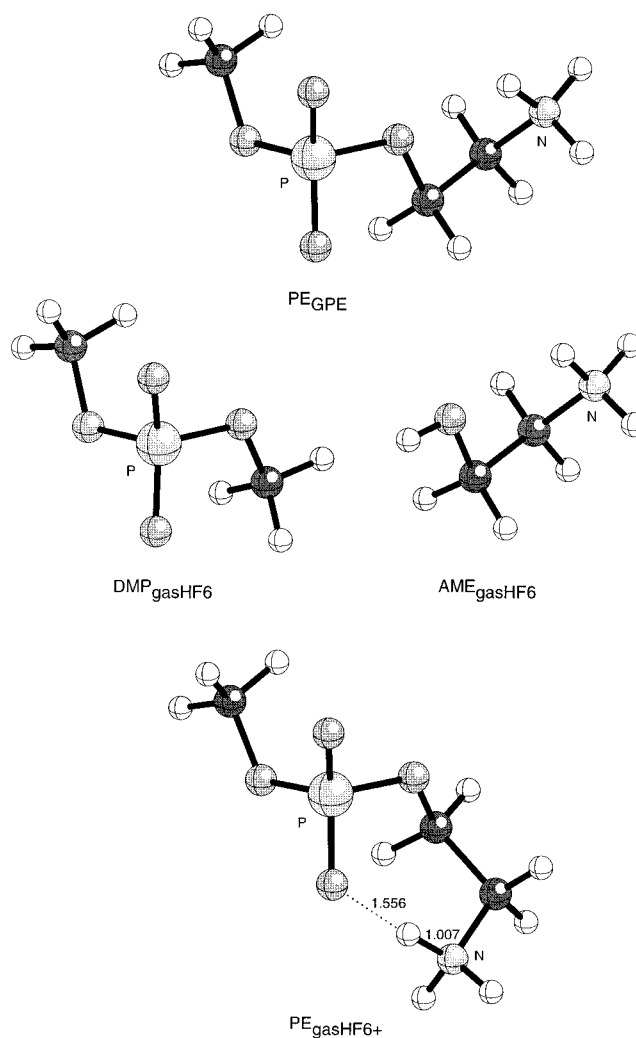


Figure 3. Crystal conformer PE_{GPE} and gas-phase minimum conformations for the molecular components DMP_{gasHF6} (dimethylphosphate), AME_{gasHF6} (2-ammonioethanol), and the whole head group, PE_{gasHF6+}. The strong attraction between the anionic and cationic parts of PE_{gasHF6+} is indicated by a dotted line. For dihedral angles see Table 2.

a cyclic conformer (PE_{solcycHF6+}) with stable zwitterionic structure. As can be seen in Table 5, the geometry of this conformer is largely unaffected by changes of the dielectric constant. Figure 6 shows that the cyclic conformer in a polar environment (PE_{solcycHF6+}) is rather similar to the constrained gas-phase conformer, PE_{gasHF6+}, revealing a close approach of the anionic phosphate oxygen and the nitrogen-bonded hydrogen. At $\epsilon = 10$, the PO...HN distance is 1.593 Å and increases with increasing polarity of the medium up to 1.633 Å at $\epsilon = 80$ (water). This should be compared to the sum of the van der Waals radii of oxygen (1.52 Å) and hydrogen (1.2 Å), which is

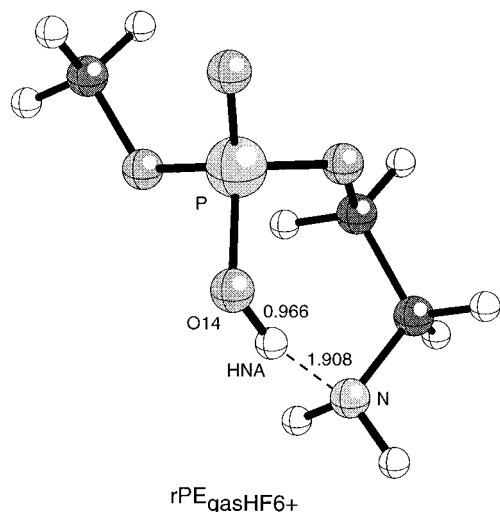


Figure 4. Gas-phase minimum conformation $rPE_{\text{gasHF6+}}$. Electrostatic interactions (with some small covalent contribution) are indicated by a dashed line. For dihedral angles see Table 2.

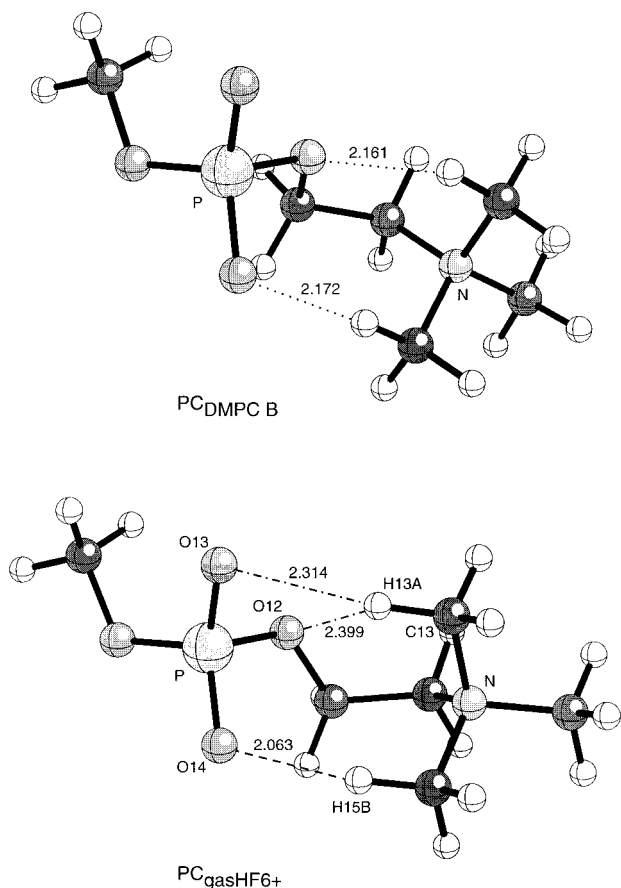


Figure 5. Crystal conformer PC_{DMPC_B} and gas-phase minimum conformation $PC_{\text{gasHF6+}}$. Short contacts in the crystal conformer are indicated by dotted lines. Electrostatic interactions (with some small covalent contribution) in the gas-phase structure are indicated by a dashed line and pure electrostatic attractions by dash-dotted lines. For dihedral angles see Table 2.

2.72 Å. Only α_2 of the dihedral angles is slightly affected by the polarity increase, changing from -74.6° ($\epsilon = 10$) to -72.4° ($\epsilon = 80$), while the remaining geometry parameters are unaffected.

The extended minimum energy conformer $PE_{\text{solextHF6+}}$ (Figure 6) is more sensitive to the polarity of the medium. Dihedral angle α_4 changes from 150.0° ($\epsilon = 10$) to 141.9° ($\epsilon = 80$), while α_5 turns in the opposite direction from 55.9° ($\epsilon = 10$) to

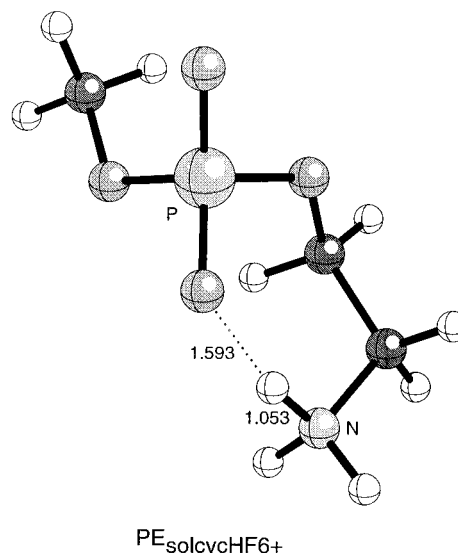
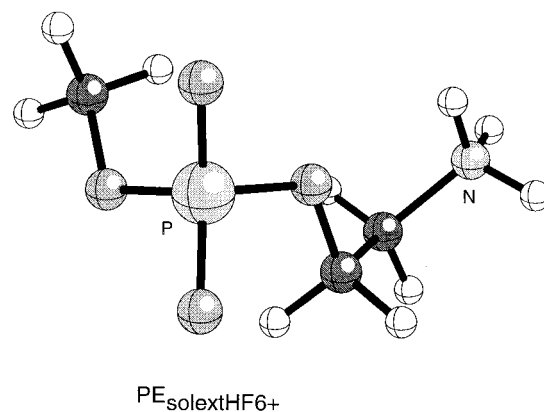


Figure 6. Optimized conformations at $\epsilon = 10$ of the extended and cyclic phosphoethanolammonium (PE) head groups. The strong attraction between the anionic and cationic parts of $PE_{\text{solcycHF6+}}$ is indicated by a dotted line. For dihedral angles see Table 5.

66.9° ($\epsilon = 80$). The dihedrals α_2 and α_3 of the phosphate group are little or not affected by polarity changes. The relative energies of the extended and cyclic PE conformers also depend on the polarity of the environment. In all cases, the cyclic conformer ($PE_{\text{solcycHF6+}}$) has the lower energy; however, at $\epsilon = 80$ the difference is only 1.6 kcal/mol.

In the presence of a polar surrounding the PC zwitterion also adopts a cyclic conformation ($PC_{\text{solcycHF6+}}$) when the gas-phase structure is used as the starting geometry. This PC conformation is rather compact, although the ring-closing oxygen to hydrogen distances are 2.4–2.5 Å, which is longer than in the gas phase, but still shorter than the sum of the van der Waals radii (2.72 Å). In contrast to PE, however, the cyclic conformer $PC_{\text{solcycHF6+}}$ is higher in energy than the extended PC conformer, $PC_{\text{solextHF6+}}$. Already at $\epsilon = 10$ the difference is 2.3 kcal/mol and can be expected to be even larger in a medium with higher dielectric constant. The preference for the extended PC conformation is supported by high-resolution NMR spectra by Hauser and co-workers, which show that the PC head group has a distinct preferred conformation with α_4 in the range 150 – 160° and $\alpha_5 \pm \textit{gauche}$, both in solution and in lipid aggregates.⁴⁵

4. Chemical Relevance and Conclusions

The objective of the present work was to explore the energetics responsible for the striking conformational similarity

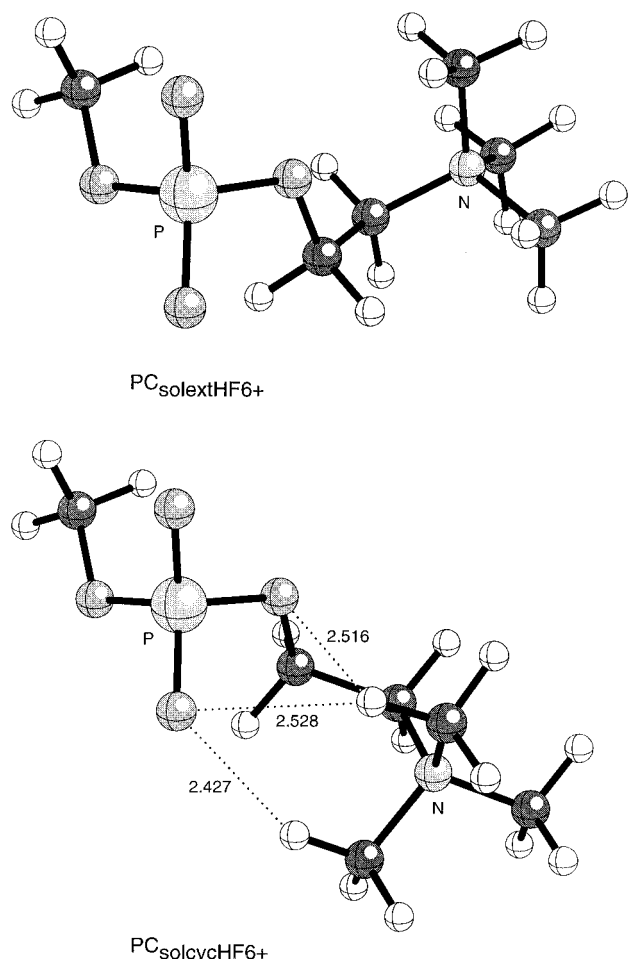


Figure 7. Optimized conformations at $\epsilon = 10$ of the extended and cyclic phosphocholine (PC) head groups. The strong attractions between the anionic and cationic parts of PC_{solcyc}HF6⁺ are indicated by dotted lines. For dihedral angles see Table 5.

of zwitterionic head groups of phosphoethanolamine (PE) and phosphocholine (PC) lipids observed in crystal structures.

Ab initio calculations show that without influence from a polar environment, i.e. in the gas phase, the positive-charged ammonium or choline group of the PE/PC head group interacts intramolecularly with one of the unesterified phosphate oxygens, giving rise to a cyclic minimum energy conformation, which differs from the preferred extended conformation observed in crystal structures.

Surprisingly, the PE zwitterion is found to be unstable in the gas phase and to convert into a neutral structure by an intramolecular proton transfer from the ammonium group to one of the phosphate oxygens. On the other hand, a relatively low dielectric constant ($\epsilon = 10$) is sufficient to block this H⁺ transfer.

Onsager calculations carried out to determine effects of the surrounding medium on conformational stabilities show that the zwitterionic, cyclic conformers of PE and PC found in the gas phase are stable conformations also in a polar environment. However, already in a medium of modest polarity ($\epsilon = 10$), a second energy minimum for an extended conformer appears. Moreover, as the polarity of the medium increases, the conformational stability of this extended conformer increases faster than that of the cyclic conformer. Interestingly, the geometry of this extended conformer, which lies within the narrow range of observed crystal conformers, is practically identical for both PE and PC and largely independent of the dielectric constant. Only with respect to the O–C–C–N bond (α_5) does PC show a 11° larger torsion angle (Table 5).

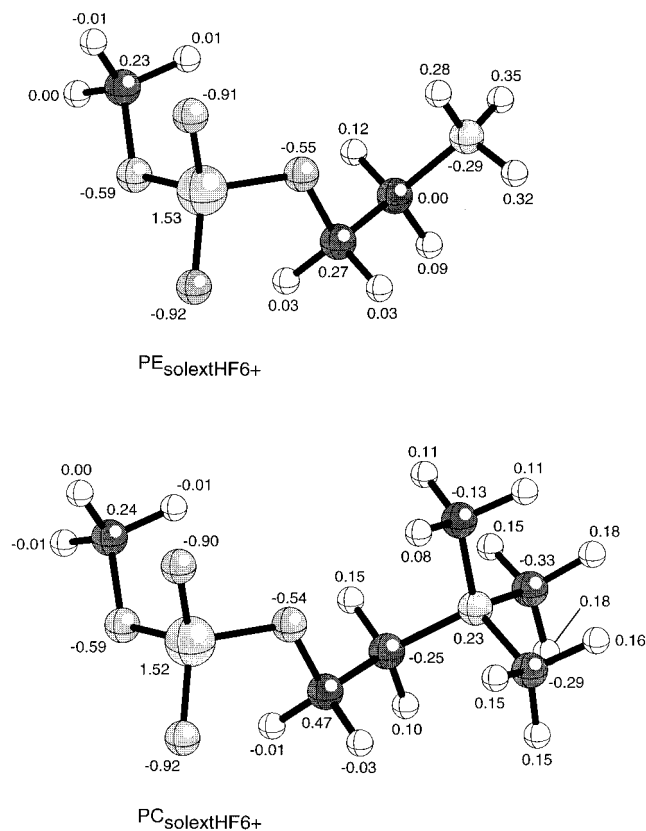


Figure 8. Partial charges at $\epsilon = 10$ for the extended phosphoethanolamine (PE) and phosphocholine (PC) head groups. For dihedral angles see Table 5.

This similarity in conformation of the PE and PC head groups in a polar environment is in line with NMR data by Akutsu and Kyogoku, which also indicate that the only significant difference between the PE and PC head groups in aqueous solution is a somewhat increased α_5 torsion in PC.⁴⁶ The difference in the α_5 torsional angle was also found by Woolf and Roux with force-field calculations on PE and PC head groups in bulk water.¹⁶ From the force-field results Woolf and Roux conclude that the difference in α_5 originates from different hydration structures around the two head groups. Our present results, however, suggest that the geometry difference originates from properties intrinsic to the molecules since the simulations were performed in a polar continuum and not with explicit water molecules. The calculations reveal a significant difference with respect to the charge distributions at the nitrogen atom of the PE and PC zwitterion. The partial charges are very similar for all corresponding atoms except for those involved in the α_5 dihedral angle, where the C12–N bond is polarized in opposite directions in the two head groups (Figure 8).

Noteworthy, the molecular dynamics study by Woolf and Roux suggests that the O–C–C–N bond, besides the characteristic \pm synclinal conformation, also adopts a remarkably high fraction of antiperiplanar conformation for both PE (31%) and PC (4%). This α_5 antiperiplanar conformer has so far not been observed in crystal structures,⁹ and although NMR data do not rule out the existence of a minor fraction of antiperiplanar conformers, the α_5 \pm synclinal conformers are reported to be the overwhelmingly dominating structures in solution and aqueous dispersions.^{45–47}

With regard to stability of the extended versus cyclic conformation the Onsager solvation model shows significant differences for PE and PC. For PC, the extended conformer has lower energy (–2.4 kcal/mol) than the cyclic conformer already at $\epsilon = 10$. For PE, on the other hand, the cyclic

conformer is energetically in preference to the extended conformer over the whole polarity range. The energy difference between the cyclic and the extended conformer, however, is rather small and decreases from 5.5 kcal/mol at $\epsilon = 10$ to only 1.6 kcal/mol at $\epsilon = 80$ (cf. Table 5).

The preference for the cyclic PE conformer in the monomeric state reflects the strong contribution of the intramolecular ammonium–phosphate interaction to the stabilization of this conformer. For ionic bonds in ammonium–phosphate complexes, interaction energies in the range 69–85 kcal/mol have been reported.^{48,49} Theoretically, the increase in $\text{PO}^{(-)}\cdots\text{N}^{(+)}$ distance from 2.5 Å in the cyclic to 5 Å in the extended conformer would reduce this interaction energy by a factor of 4. Considering this anticipated effect of charge separation, the observed differences in conformational energy between the cyclic and extended conformer are remarkably small. This indicates that the extended conformation, despite the lack of an explicit intramolecular ionic bond, is already stabilized in the monomeric state by energetics intrinsic to the phosphoethanolammonium backbone and that the transformation to the cyclic conformation is accompanied by a considerable steric strain.

The intrinsic stability of the extended conformer is supported by results from gas-phase ab initio calculations on the PE substructures dimethylphosphate (DMP) and 2-ammonioethanol (AME).¹⁷ If the phosphoethanolammonium zwitterion is divided into the (–) and the (+) charged fragment, devoid of strains from an intramolecular ionic interaction, the two fragments adopt minimum energy torsions (cf. Table 2) which are in full agreement with those of the extended conformer of the PE/PC head group in solution or in crystals. Furthermore, for the AME part this minimum conformer is located in a potential well which restricts the α_4 dihedral to an antiperiplanar and α_5 to either one of the \pm synclinal positions (cf. Figure 7c in ref 17). Although it is appealing to draw conclusions from the above, one should keep in mind that these results are from gas-phase calculations on head group substructures.

In the cyclic zwitterionic PE structure the intramolecular ionic interaction forces the α_4/α_5 dihedrals out of the potential well, primarily by turning α_4 (+124°) from the favored *ac/ap* (150°) range to the *–ac/–sc* (–86°) range (see Table 5, $\epsilon = 10$). To a minor extent the cyclization also affects the adjacent torsions α_3 (+18°) and α_5 (+23°). For the cyclization of PC the corresponding changes of the torsion angles α_3 (+14°), α_4 (+75°), and α_5 (+6°) are less pronounced.

While for PC in the monomeric state the intramolecular ionic interaction is balanced by intermolecular polar interactions already at $\epsilon < 10$, for PE the applied continuum method suggests that the cyclic conformer is favored (–1.6 kcal/mol) over the extended structure also at $\epsilon = 80$. Experimental observations from NMR analysis, however, indicate that both PC and PE in D_2O , CD_3OD , and CDCl_3 solutions adopt the characteristic extended conformation, possibly with some distortion of PE in CDCl_3 .⁴⁶ For PE in lipid aggregates, on the other hand, there is evidence from deuterium NMR that, for example, in lipid bilayers the intramolecular ionic bond of the cyclic PE head group will be replaced by cooperative intermolecular ammonium \cdots phosphate interactions favoring the extended conformation,¹⁰ thereby combining the stabilizing factors of the two PE conformations from the monomeric state. These intermolecular interactions are also distinctly manifested in the solid state by X-ray structure determinations.⁹ Also, recent molecular dynamics simulations of PE membrane domains^{50–52} have demonstrated that intermolecular ionic interactions take place

between neighboring lipid head groups and are important stabilizing factors in dynamic bilayers.

The intrinsic stability of the extended minimum energy conformer of PE/PC head groups and its favorable stabilization in aggregated lipid phases thus can explain the predominance of this conformer in crystal structures,⁹ aqueous dispersions, and biomembranes.¹⁰

Acknowledgment. This work was supported by the Swedish Medical Research Council (MFR, Grant 0006) and the Swedish Natural Science Research Council (NFR). The calculations were done on the CRAY X-MP/416 and the Cray Y-MP/464 of the Nationellt Superdatorcentrum (NSC), Linköping, Sweden, and on a Silicon Graphics Challenge server at the MEDNET laboratory. The authors thank the NSC for a generous allotment of computer time and the Skandinaviska Enskilda Bankens Foundation for a generous grant for computer equipment. Useful discussions with Staffan Sundell, Department of Medical Biochemistry, and Lars Olsson and Henrik Ottosson from the Department of Theoretical Chemistry are acknowledged.

Supporting Information Available: Tables of absolute energies and coordinate files for the 11 most important conformers (13 pages). Ordering information is given on any current masthead page.

References and Notes

- (1) *Introduction to Biological Membranes*; Jain, M. K., Wagner, R. C., Eds.; John Wiley & Sons: New York, 1980.
- (2) Janiak, M. J.; Small, D. M.; Shipley, G. G. *J. Biol. Chem.* **1979**, *254*, 6068–6078.
- (3) *Physical Chemistry of Lipids*; Small, D. M., Ed.; Plenum Press: New York, 1986; pp 475–522.
- (4) Seddon, J. M. *Biochim. Biophys. Acta* **1990**, *1031*, 1–69.
- (5) Cullis, P. R.; Hope, M. J.; Tilcock, C. P. S. *Chem. Phys. Lipids* **1986**, *40*, 127–144.
- (6) Cullis, P. R.; Hope, M. J.; de Kruijff, B.; Verkleij, A. J.; Tilcock, C. P. S. In *Phospholipids and Cellular Regulations*; Kuo, J. F., Ed.; CRC Press: Boca Raton, 1985; Vol. 1, pp 1–59.
- (7) Zachowski, A. *Biochem. J.* **1993**, *294*, 1–14.
- (8) Zachowski, A.; Favre, E.; Cribier, S.; Hevré, P.; Devaux, P. F. *Biochemistry* **1986**, *25*, 2585–2590.
- (9) Pascher, I.; Lundmark, M.; Nyholm, P.-G.; Sundell, S. *Biochim. Biophys. Acta* **1992**, *1113*, 339–373.
- (10) Seelig, J. *Q. Rev. Biophys.* **1977**, *10*, 353–418.
- (11) Pullman, B.; Berthod, H. *FEBS Lett.* **1974**, *44*, 266–269.
- (12) Pullman, B.; Berthod, H.; Gresh, N. *FEBS Lett.* **1975**, *53*, 199–204.
- (13) Pullman, B.; Saran, A. *Int. J. Quantum Chem.: Quantum Biol. Symp.* **1975**, 71–97.
- (14) Frischleder, H.; Peinel, G. *Chem. Phys. Lipids* **1982**, *30*, 121–158.
- (15) Frischleder, H.; Lochmann, R. *Int. J. Quantum Chem.* **1979**, *16*, 203–213.
- (16) Woolf, T. B.; Roux, B. *J. Am. Chem. Soc.* **1994**, *116*, 5916–5926.
- (17) Landin, J.; Pascher, I.; Cremer, D. *J. Phys. Chem.* **1995**, *99*, 4471–4485.
- (18) Wong, M. W.; Frisch, M. J.; Wiberg, K. B. *J. Am. Chem. Soc.* **1991**, *113*, 4776–4782.
- (19) Wong, M. W.; Wiberg, K. B.; Frisch, M. J. *J. Am. Chem. Soc.* **1992**, *114*, 523–529.
- (20) Wong, M. W.; Wiberg, K. B.; Frisch, M. J. *J. Am. Chem. Soc.* **1992**, *114*, 1645–1652.
- (21) Wong, M. W.; Wiberg, K. B.; Frisch, M. J. *Chem. Phys.* **1991**, *95*, 8991–8998.
- (22) Frisch, M. J.; Head-Gordon, M.; Trucks, G. W.; Foresman, J. B.; Schlegel, H. B.; Raghavachari, K.; Robb, M.; Binkley, J. S.; Gonzalez, C.; Defrees, D. J.; Fox, D. J.; Whiteside, R. A.; Seeger, R.; Melius, C. F.; Baker, J.; Martin, R. L.; Kahn, L. R.; Stewart, J. J. P.; Topiol, S.; Pople, J. A. *Gaussian 90*; Revision F; Gaussian, Inc.: Pittsburgh, PA, 1990.
- (23) Frisch, M. J.; Trucks, G. W.; Schlegel, H. B.; Gill, P. M. W.; Johnson, B. G.; Wong, M. W.; Foresman, J. B.; Robb, M. A.; Head-Gordon, M.; Replogle, E. S.; Gomperts, R.; Andres, J. L.; Raghavachari, K.; Binkley, J. S.; Gonzalez, C.; Martin, R. L.; Fox, D. J.; Defrees, D. J.; Baker, J.; Stewart, J. J. P.; Pople, J. A. *Gaussian 92/DFT*, Revision F.3; Gaussian, Inc.: Pittsburgh, PA, 1993.

- (24) Kraka, E.; Gauss, J.; Reichel, F.; He, Z.; Konkoli, Z.; Olsson, L.; Cremer, D. *COLOGNE 94*; University of Göteborg: Sweden, 1994.
- (25) Binkley, J. S.; Pople, J. A.; Hehre, W. J. *J. Am. Chem. Soc.* **1980**, *102*, 939–947.
- (26) Gordon, M. S.; Binkley, J. S.; Pople, J. A.; Pietro, W. J.; Hehre, W. J. *J. Am. Chem. Soc.* **1982**, *104*, 2797–2803.
- (27) Pietro, W. J.; Francl, M. M.; Hehre, W. J.; Defrees, D. J.; Pople, J. A.; Binkley, J. S. *J. Am. Chem. Soc.* **1982**, *104*, 5039–5048.
- (28) Hehre, W. J.; Ditchfield, R.; Pople, J. A. *J. Chem. Phys.* **1972**, *56*, 2257–2261.
- (29) Hariharan, P. C.; Pople, J. A. *Theor. Chim. Acta* **1973**, *28*, 213–222.
- (30) Gordon, M. S. *Chem. Phys. Lett.* **1980**, *76*, 163–168.
- (31) Frisch, M. J.; Pople, J. A.; Binkley, J. S. *J. Chem. Phys.* **1984**, *80*, 3265–3269.
- (32) Clark, T.; Chandrasekhar, J.; Spitznagel, G. W.; Schleyer, P. v. R. *J. Comput. Chem.* **1983**, *4*, 294–301.
- (33) Minkin, V. I.; Simkin, B. Y.; Minyaev, R. M. In *Quantum Chemistry of Organic Compounds: Mechanisms of Reactions*; Springer-Verlag: Berlin, 1990; pp 90–92.
- (34) Minkin, V. I.; Simkin, B. Y.; Minyaev, R. M. In *Quantum Chemistry of Organic Compounds: Mechanisms of Reactions*; Springer-Verlag: Berlin, 1990; pp 88–105.
- (35) Cramer, C. J.; Truhlar, D. G. Development and Biological Applications of Quantum Mechanical Continuum Solvation Models. In *Quantitative Treatments of Solute/Solvent Interactions*, 1st ed.; Politzer, P., Murray, J. S., Eds.; Elsevier Science B. V.: Amsterdam, 1994; Vol. 1, pp 9–54.
- (36) Breneman, C. M.; Wiberg, K. B. *J. Comput. Chem.* **1990**, *11*, 361–373.
- (37) Cremer, D.; Kraka, E. *Croatica Chem. Acta* **1984**, *57*, 1259–1281.
- (38) Sundaralingam, M. *Ann. N. Y. Acad. Sci.* **1972**, *195*, 324–355.
- (39) DeTitta, G. T.; Craven, B. M. *Acta Crystallogr. B* **1973**, *29*, 1354–1357.
- (40) Hauser, H.; Pascher, I.; Pearson, R. H.; Sundell, S. *Biochim. Biophys. Acta* **1981**, *650*, 21–51.
- (41) Bondi, A. *J. Phys. Chem.* **1964**, *68*, 441–451.
- (42) Frisch, M. J.; Head-Gordon, M.; Pople, J. A. *Chem. Phys. Lett.* **1990**, *166*, 281–289.
- (43) Spitznagel, G. W.; Clark, T.; Chandrasekhar, J.; Schleyer, P. v. R. *J. Comput. Chem.* **1982**, *3*, 363–371.
- (44) Chandrasekhar, J.; Andrade, J. G.; Schleyer, P. v. R. *J. Am. Chem. Soc.* **1981**, *103*, 5609–5612.
- (45) Hauser, H.; Guyer, W.; Pascher, I.; Skrabal, P.; Sundell, S. *Biochemistry* **1980**, *19*, 366–373.
- (46) Akutsu, H.; Kyogoku, Y. *Chem. Phys. Lipids* **1977**, *18*, 285–303.
- (47) Akutsu, H. *Biochemistry* **1981**, *20*, 7359–7366.
- (48) Prasad, C. V.; Pack, G. R. *J. Am. Chem. Soc.* **1984**, *106*, 8079–8086.
- (49) Deerfield, D. W. I.; Nicholas, H. B. J.; Hiskey, R. G.; Pedersen, L. G. *Proteins: Struct., Funct., Genet.* **1989**, *6*, 168–192.
- (50) Damodaran, K. V.; Merz, K. M.; Gaber, B. P. *Biochemistry* **1992**, *31*, 7656–7664.
- (51) Damodaran, K. V.; Merz, K. M. *Biophys. J.* **1994**, *66*, 1076–1087.
- (52) Huang, P.; Perez, J. J.; Loew Gilda, H. *J. Biomol. Struct. Dyn.* **1994**, *11*, 927–956.